

Wenbin Zhao

# **Computational Physics: Static Quark Potential of SU(2) Theory**

24 March 2020

Tutors: Prof. Carsten Urbach

Universität Bonn

# Contents

<b>1</b>	<b>Introduction</b>	<b>1</b>
<b>2</b>	<b>Minimum Lattice Gauge Theory</b>	<b>2</b>
2.1	From Minkowski space to Euclidean space . . . . .	2
2.2	Lattice Action . . . . .	3
2.3	Wilson Loops . . . . .	5
<b>3</b>	<b>Simulation Techniques</b>	<b>7</b>
3.1	Realisation of Gauge Link Variables . . . . .	7
3.2	The Monte Carlo method . . . . .	7
3.3	Metropolis algorithm for Pure Gauge Action . . . . .	7
3.4	Autocorrelation and Bootstrap . . . . .	10
<b>4</b>	<b>Simulation Results and Conclusion</b>	<b>11</b>
4.1	Wilson Loop . . . . .	11
4.2	Static Quark Potential . . . . .	12
<b>5</b>	<b>Summary</b>	<b>13</b>

# 1 Introduction

Quark confinement is a famous feature of QCD theory, which says that there is no free quark can be observed. In 1974, Wilson proved that in strong coupling limit (where coupling constant is taken to be infinity), the confinement exist. But the general proof is hard to give since the confinement shows in non-perturbative region. Thus we can only study that with the help of numerical simulation.

In this project, we study the static quark potential under  $SU(2)$  Yang-Mills Theory. The static means quarks are infinity heavy. We show that the potential between quark-antiquark pairs grows with increasing distance, which can be regarded as an evidence of confinement.

The following methods are used in this project to get the final results:

- Monte-Carlo Integration to relate Field Theory and simulation.
- Metropolis algorithm to generate desired configuration space.
- Bootstrap methods to go against the high auto-correlation between generated configurations.

In section 2 we give a short introduction to Gauge Theory. Computer can only deal with discrete case, so we have to move our theory from Minkowski space to a lattice space. Then we discuss simulation techniques mentioned above in section 3. Since all the readers are supposed to already know them in the CPP course, we will focus on how to apply them in gauge theory. The results is discussed in section 4 and we give a short summary in section 5. The project is realised on Python and can be reached by <https://github.com/compphys-unibonn-2019/wenbin-zhao>.

## 2 Minimum Lattice Gauge Theory

There are three key points for a lattice gauge theory:

- We work in Euclidean space instead of Minkowski space.
- We will put every thing on discrete coordinate system, or say, the lattice.
- The gauge invariance should be preserved.

One may wonder why we give up the Lorentz invariance so easily but try to maintain the gauge invariance really hard. The point is that gauge invariance make sure all the coupling constant in our theory (such as quark-gluon vertex and 3/4 point gluon vertex) are same, which will simplify our life. This chapter strongly follows [1], chapter 2 and 3.

### 2.1 From Minkowski space to Euclidean space

We apply wick rotation to our coordinate. The introduction to wick rotation can be found in any QFT book, we will not go through that here. After wick rotation, the zero component of coordinates and momentum changes follow:

$$\begin{aligned}x_0 = t &\mapsto -i\tau \\ p_0 = E &\mapsto -iE\end{aligned}\tag{2.1}$$

In minkowski space, the two point function of any operator can be defined as

$$\langle \hat{O}_1 \hat{O}_2 \rangle = Z_M^{-1} \int D[A_\mu] D[\psi] D[\bar{\psi}] O_1 O_2 e^{-iS_M}\tag{2.2}$$

Where  $Z_M$  is the normalisation factor, which is same expression with out operator  $O_1$  and  $O_2$ .  $S_M$  is the action.  $O_1$  and  $O_2$  are general operator built by fermion and gauge field. Here we use subscript M to donate Minkowski space. After wick rotation, the two point function changes to

$$\langle \hat{O}_1 \hat{O}_2 \rangle = Z_E^{-1} \int D[A_\mu] D[\psi] D[\bar{\psi}] O_1 O_2 e^{-S_E}\tag{2.3}$$

Here we get a Gaussian-like weight factor  $e^{-S_E}$ , which is suitable to apply Monte-Carlo method.

## 2.2 Lattice Action

A typical lattice has a spacing  $a$  and length  $L$  (related with the total number of points), the spacing  $a$  provides a UV cutoff and  $L$  gives a IR cutoff. We get the continue limit when  $a \rightarrow 0$ . In principle, the IR cutoff should below the mass of pion and UV cutoff should be higher than what we interest.

Another thing we have to remark is spacing  $a$  is not a input parameter, instead we set coupling  $g$ . Due to running coupling of QCD,  $a$  and  $g$  is related and  $a$  can be determined later. In this project we won't counter this problem.

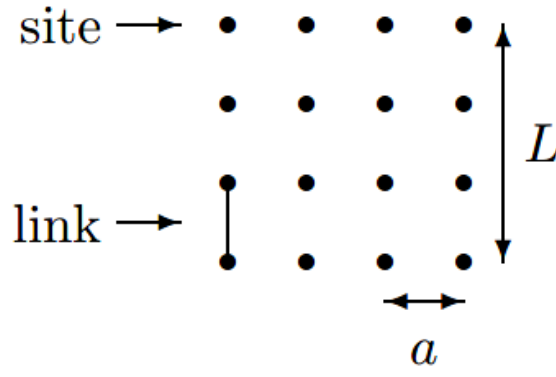


**Figure 2.1:** a lattice with spacing  $a$  and length  $L$ , quarks live in each point and glouns(link) live between two points,taken from [2].

Now we are ready to put fermion fields on our lattice point,

$$\psi(n) \quad \bar{\psi}(n) \quad n_\mu = 0, 1, \dots, L \quad \mu = 0, 1, 2, 3 \quad (2.4)$$

The free fermion part action reads

$$S_F^0[\bar{\psi}, \psi] = \int d^4x \bar{\psi}(x)(\gamma_\mu \partial^\mu + m)\psi(x) \quad (2.5)$$

To get the discrete form, the  $\int d^4x$  changes to sum of all points, the  $\partial$  changes to finite difference:

$$S_F^0[\bar{\psi}, \psi] = a^4 \sum_n \bar{\psi}(n) \left( \sum_\mu \gamma_\mu \frac{\psi(n + \hat{\mu}) - \psi(n - \hat{\mu})}{2a} + m\psi(n) \right) \quad (2.6)$$

Keep in mind that  $\psi$  is still grassmann numbers and since we use different metric tensor the  $\gamma$  matrix is different with ordinary one. The gauge transformation of fermion field is

$$\psi(n) \rightarrow V(n)\psi(n) \quad \bar{\psi}(m) \rightarrow \bar{\psi}(m)V^\dagger(m) \quad V(n) \in SU(2) \quad (2.7)$$

The bilinear term  $\bar{\psi}(m)\psi(n)$  is not invariant since  $V(n)$  and  $V(m)$  is not the same matrix. To make the bilinear term gauge invariant, we introduce the so called gauge Link variables, connecting the quark-antiquark pair, which is

$$\bar{\psi}(m)U(m,n)\psi(n) \equiv \bar{\psi}(m)(Pe^{\int_n^m igA_\mu(x)dx_\mu})\psi(n) \quad (2.8)$$

The right hand side is the continue case, which we do not need actually. The transformation property of link variables  $U(m,n)$  is

$$U(m,n) \rightarrow V(m)U(m,n)V^\dagger(n) \quad (2.9)$$

which makes the bilinear term  $\bar{\psi}(m)U(m,n)\psi(n)$  indeed invariant. The link variables plays a crucial important role in our project.

The link variables of length 1 is the basement of theory, we define

$$U(m, m + \hat{\mu}) \equiv U_\mu(m) \quad (2.10)$$

So the link variables is defined on the 4 directions of each point. We can also define the inverse link variables, they are defined as the conjugate of the positive one.

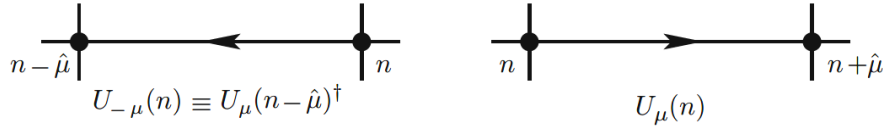


**Figure 2.2:** The link variables of  $U_\mu$  and  $U_{-\mu}$ , taken from [1].

We can now build a gauge invariant action:

$$S_F[\bar{\psi}, \psi, U] = a^4 \sum_n \bar{\psi}(n) \left( \sum_\mu \gamma_\mu \frac{U_\mu(n)\psi(n + \hat{\mu}) - U_{-\mu}(n)\psi(n - \hat{\mu})}{2a} + m\psi(n) \right) \quad (2.11)$$

One can easily check  $S_F[\bar{\psi}, \psi, U] = S_F[\bar{\psi}', \psi', U']$  under (2.7) and (2.9). But we still need to put kinetic term of gauge field in our Lagrangian.

The kinetic term can be constructed by the so-called plaquette term, this is the smallest gauge invariant object we can get without fermion fields.

$$\begin{aligned} U_{\mu\nu}(n) &= U_\mu(n)U_\nu(n + \hat{\mu})U_{-\mu}(n + \hat{\mu} + \hat{\nu})U_{-\nu}(n + \hat{\nu}) \\ &= U_\mu(n)U_\nu(n + \hat{\mu})U_\mu^\dagger(n + \hat{\nu})U_\nu^\dagger(n) \end{aligned} \quad (2.12)$$

The Wilson gauge action is then defined as:

$$S_G[U] = \frac{2}{g^2} \sum_{n \in \Lambda} \sum_{\mu < \nu} \text{Re Tr}(1 - U_{\mu\nu}(n)) \quad (2.13)$$

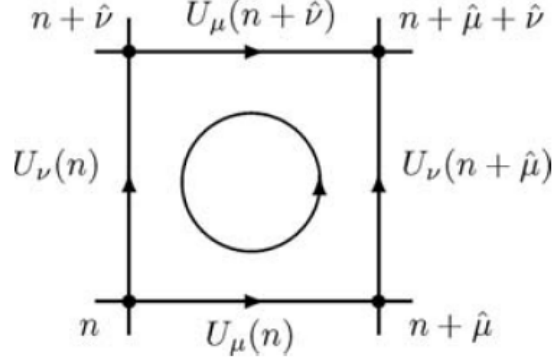


**Figure 2.3:** The plaquette built by 4 link variables, the circle means the order of link variables when they are multiplied. taken from [1].

We may rewrite the action by

$$S_G[U] = \frac{\beta}{N} \sum_{n \in \Lambda} \sum_{\mu < \nu} \text{Re Tr}(1 - U_{\mu\nu}(n)) \quad (2.14)$$

Here  $\beta = \frac{2N}{g^2}$  is called inverse coupling,  $N$  means we use the  $SU(N)$  gauge group in our theory. One can prove that the clockwise product of link variables is just the complex conjugate of the counterclockwise one. By taking the real part of the trace we actually average the contribution of both cases. In the  $a \rightarrow 0$  limit, this action will reduce to the continue one. By (2.8) and Baker-Campbell-Hausdorff formula, we can show:

$$\frac{2}{g^2} \sum_{n \in \Lambda} \sum_{\mu < \nu} \text{Re Tr}(1 - U_{\mu\nu}(n)) = \frac{a^4}{2g^2} \sum_{n \in \Lambda} \sum_{\mu < \nu} \text{Re Tr}(F_{\mu\nu}(n)^2) \quad (2.15)$$

The coupling shows in the denominator simply because we put factor 1 in front of coupling between  $U$  and  $\psi$  field in (2.11), we can rescale  $A_\mu \rightarrow gA_\mu$  so the factor  $g^2$  will disappear from our expression, and the Lagrangian goes back to our familiar form.

## 2.3 Wilson Loops

Since all the physical observables should be gauge invariant, we would like to focus on the gauge-invariant object made from only gauge fields. A typical object is the Wilson Loop.

A Wilson loop  $W_L$  is built by 4 pieces, 2 space lines and 2 time lines. The space line  $S(m, n, n_t)$  is also called Wilson line, which connects two spatial points  $\vec{m}$  and  $\vec{n}$  by some path  $L_{m,n}$  with the same time argument  $n_t$ .  $(\vec{m}, n_t) \rightarrow (\vec{n}, n_t)$

$$S(\vec{m}, \vec{n}, n_t) = \prod_{(\vec{k}, j) \in L_{\vec{m}, \vec{n}}} U_j(\vec{k}, n_t) \quad (2.16)$$

The time line is just a straight line in time direction with length  $n_t, (\vec{n}, 0) \rightarrow (\vec{n}, n_t)$

$$T(\vec{n}, n_t) = \prod_{j=0}^{n_t-1} U_0(\vec{n}, j) \quad (2.17)$$

To get a closed loop, we also need a inverse space line form  $(\vec{n}, 0) \rightarrow (\vec{m}, 0)$  and time line from  $(\vec{m}, n_t) \rightarrow (\vec{m}, 0)$ . The Wilson Loop  $W_L$  is the trace of the product of these four pieces:

$$W_L[U] = \text{tr}[S(\vec{m}, \vec{n}, n_t) T(\vec{n}, n_t)^\dagger S(\vec{m}, \vec{n}, 0)^\dagger T(\vec{m}, n_t)] \quad (2.18)$$

If the space line is a straight line, the Wilson loop is planar. Otherwise it is called nonplanar. The Wilson line is directly related to the static quark potential, one can show [1] that for large

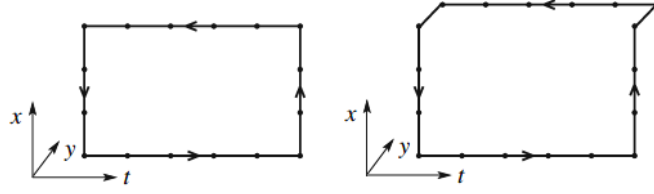


**Figure 2.4:** Examples of a planar and nonplanar Wilson loop. [1].

$t = an_t$ :

$$\langle W_L(r, t) \rangle \propto \exp(-an_t V(r)) \quad (2.19)$$

Thus we can get the potential by

$$\langle aV(r) \rangle = \ln \frac{\langle W_L(r, t) \rangle}{\langle W_L(r, t+1) \rangle} \quad (2.20)$$

Since in strong coupling limit we will get linear rising potential and in small coupling we get coulomb potential, we will parameterize the static potential by

$$V(r) = \frac{A}{r} + B + \sigma r. \quad (2.21)$$

Here  $\sigma$  is called string tension.



# 3 Simulation Techniques

## 3.1 Realisation of Gauge Link Variables

A general SU(2) matrix can be parameterized by two complex numbers:

$$U = \begin{pmatrix} a & b \\ -b^* & a^* \end{pmatrix} \quad |a|^2 + |b|^2 = 1 \quad (3.1)$$

On each site we put 4 link variables corresponding 4 directions along the axis.

## 3.2 The Monte Carlo method

In 2.1 we already show in Euclidean space the path integral formalism can be written as

$$\langle O \rangle = Z^{-1} \int D[U] e^{-S_G[U]} O[U] \quad (3.2)$$

This integral is not analytic but one can use Monte Carlo simulation to approximate the integral by

$$\langle O \rangle \approx \frac{1}{N} \sum_{U_n} O[U_n] \quad (3.3)$$

$N$  is the size of configuration space, where  $U_n$  is distributed with the probability  $\propto e^{-S_G[U]}$ . We generate this configuration space by metropolis algorithm.

## 3.3 Metropolis algorithm for Pure Gauge Action

The general idea of metropolis algorithm is change the field configuration and accept/reject this change with a certain probability associated with the distribution we want.

For our gauge action, we can update a single link variable  $U_\mu(n) \rightarrow U_\mu(n)'$ , since our gauge action only contains the smallest Wilson loop, it will only influence 6 loop : 3 planes with 2 loops affected in each plane. So the local contribution to the action is

$$S[U_\mu(n)'] = \frac{\beta}{N} \sum_{i=1}^6 \text{Retr}[1 - U_\mu(n)' P_i] = \frac{\beta}{N} \text{Retr}[6 - U_\mu(n)' A] \quad (3.4)$$

Here  $P_i$  is products of the other three link variables and  $A$  is just sum of  $P_i$  in 3 planes.

$$A = \sum_{i=1}^6 P_i = \sum_{\nu \neq \mu} U_\nu(n + \hat{\mu}) U_{-\mu}(n + \hat{\mu} + \hat{\nu}) U_{-\nu}(n + \hat{\nu}) \\ + U_{-\nu}(n + \hat{\mu}) U_\mu(n + \hat{\mu} - \hat{\nu}) U_\nu(n - \hat{\nu}) \quad (3.5)$$

Now the change is simply

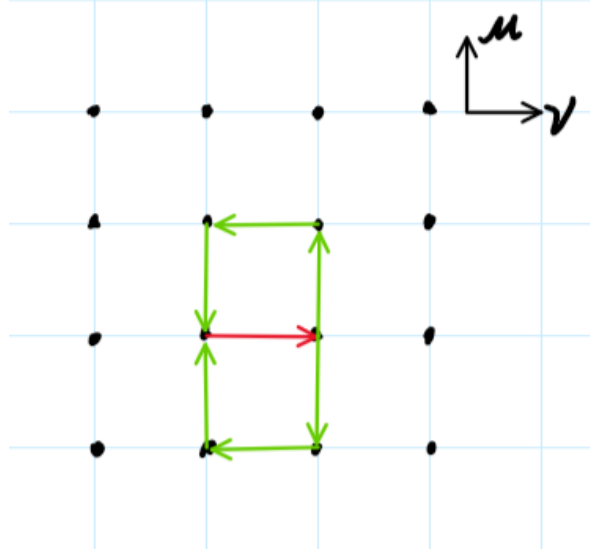


**Figure 3.1:** The local loop influenced by the update link in the  $\mu\nu$  plane, here red link is updated one and green link is not.

$$\Delta S = S[U_\mu(n)'] - S[U_\mu(n)] = -\frac{\beta}{N} \text{ReTr}[(U_\mu(n)' - U_\mu(n))A] \quad (3.6)$$

Once we calculate the change of action  $\Delta S$ , we would accept the new link variables  $U_\mu(n)'$  if we generate a random number  $r$  between  $(0,1)$  and  $r \leq \exp(-\Delta S)$ . So how we update the Link variables? Here we multiply another random SU(2) matrix  $X$ :

$$U_\mu(n)' = XU_\mu(n) \quad (3.7)$$

If  $X$  is close to Identity, we move slowly in the configuration space and the acceptance rate should be high, vice versa. So we introduce a parameter  $r$  to control the distance of our matrix to Identity in 3.1:

$$\begin{aligned} \text{Re}(a) &= \sqrt{1-r^2} & \text{Im}(a) &= x_1 & x_1^2 + x_2^2 + x_3^2 &= r^2 \\ \text{Re}(b) &= x_2 & \text{Im}(b) &= x_3 \end{aligned} \quad (3.8)$$

Here small  $r$  means close to Identity and large  $r$  means far from Identity. We show the relation between acceptance rate and distance  $r$  in 3.2.

One more thing to mention is that one can either initial our Link variables by hot( links are set to be random SU(2) matrices) or cold(set to be Identity). Cold start has an advantage that we can actually calculate the observables and compare them with simulated results. But both cold and hot star will converge to same region after Equilibration as we can see in 3.3 by plaquette expectation values, which is slightly different with gauge action:

$$\langle \text{Plaquette} \rangle = \frac{1}{N} \sum_{n \in \Lambda} \sum_{\mu < \nu} \text{Re Tr}(U_{\mu\nu}(n)) \quad (3.9)$$

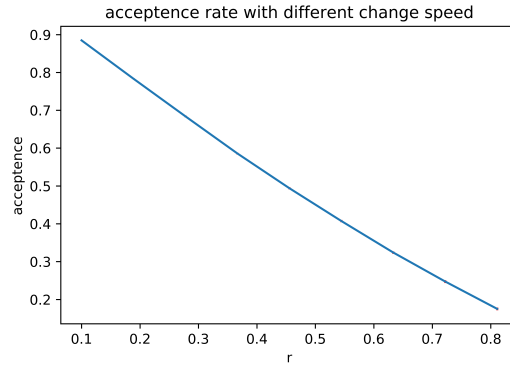


**Figure 3.2:** Acceptance rate change with parameter  $r$ , each acceptance rate is calculated after 100 update.

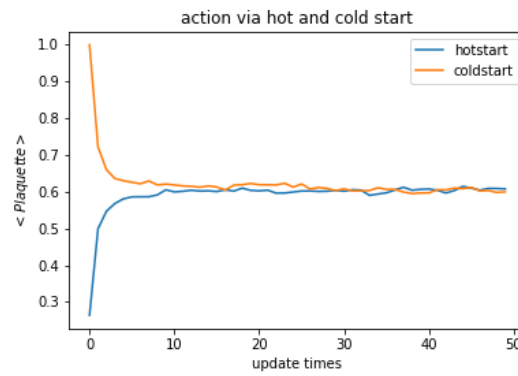


**Figure 3.3:** Plaque expectation value in different cases.

### 3.4 Autocorrelation and Bootstrap

Since we generate the link configuration by Markov chain, the configuration is actually correlated. We can see this by taking the inner product of initial Link variables with later ones. To get rid of this autocorrelation in observables, we do bootstrap to our data. Just re-sampling

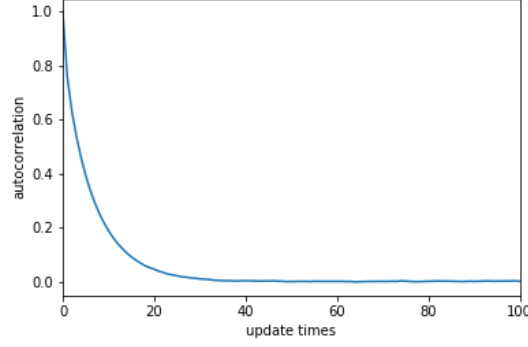


**Figure 3.4:** correlation between Link variables along the update times

the original data, in our project, which is the Wilson loop value where we get static quark potential by 2.20. Suppose we have  $N$  raw data for Wilson Loop in certain distance and different time:  $(W_n(r, 0), W_n(r, 1), \dots, W_n(r, t))$ , where  $n$  donates the results of  $n$ -th link variable configuration and we have  $N$  such results. We can replace each result by randomly choosing the results among the original results. A new raw data could be  $(W_{n'}(r, 0), W_{n''}(r, 1), \dots, W_{n'''}(r, t))$ , where  $n', n'', n''' \in (1, N)$ , we can rebuilt  $N$  datas and do this  $K$  times. Then the observables can be gotten by

$$\tilde{\theta} \equiv \frac{1}{K} \sum_{k=1}^K \theta_k, \quad \sigma_{\tilde{\theta}} \equiv \frac{1}{K} \sum_{k=1}^K (\theta_k - \tilde{\theta})^2 \quad (3.10)$$

As we can see in 3.5, the bootstrap method really increase the accuracy.

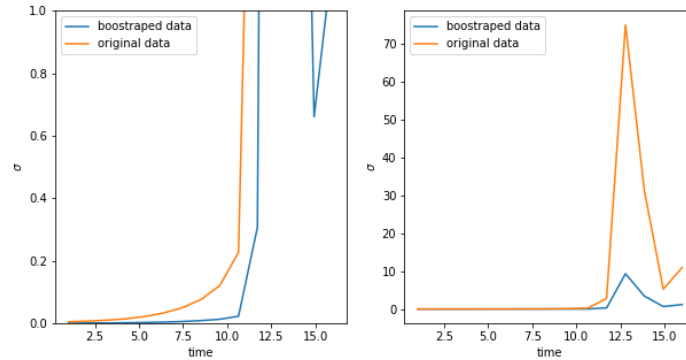


**Figure 3.5:** The standard error of static quark potential before and after bootstrap( $K=10000$ )

## 4 Simulation Results and Conclusion

We run a simulation with  $T = 32, X = Y = Z = 12, \beta = 2.3$ , the distance parameter is 0.45 with a acceptance rate 0.497(2). We generate 1k link variable configurations and discard the first 500 configurations to make sure we really go to equilibration.

### 4.1 Wilson Loop

The plaquette expectation value, defined in 3.9, is 0.6023(8), which is agree with [3]'s results 0.60227(3).

The results about Wilson Loop is in 4.1, we can see they actually decay exponentially.

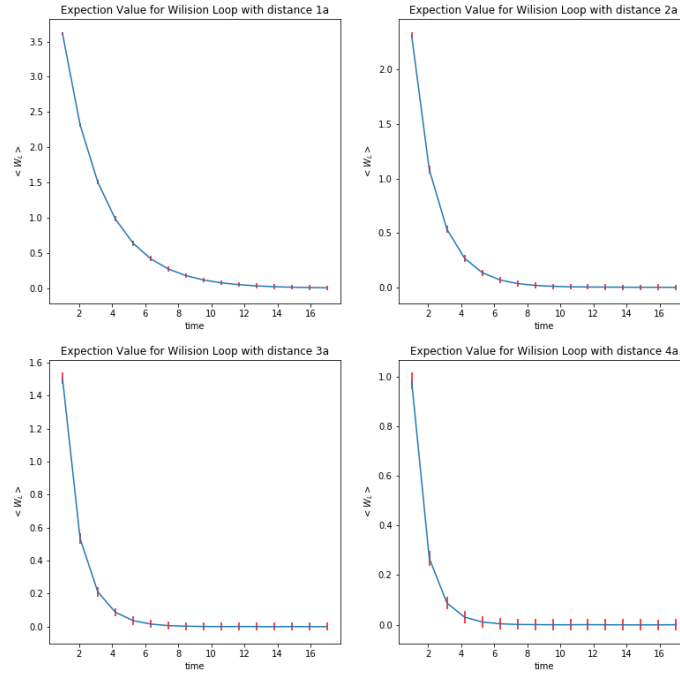


**Figure 4.1:** The expection value for Wilson loops in different distance, the error bar is  $3\sigma$  to make it more visible.

## 4.2 Static Quark Potential

The energy gotten from Wilson Loop via 2.20 is shown in 4.2. The sad thing is that our sample

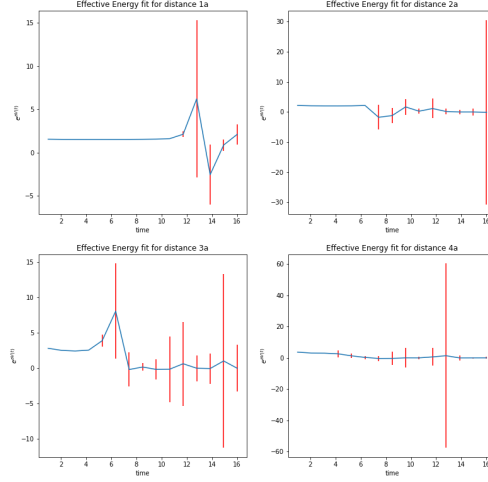


**Figure 4.2:** The potential in different time and distance.

size is not big enough so the standard error is crucially big even after the bootstrap. Since the potential is supposed to decrease to ground state, We can only choose the first non-increasing value as our results for Static Quark Potential. Here we choose  $t=3$ , which is not big enough but we do not have better choice.

The Static Quark Potential is shown in 4.3. As we can see the potential increase with distance

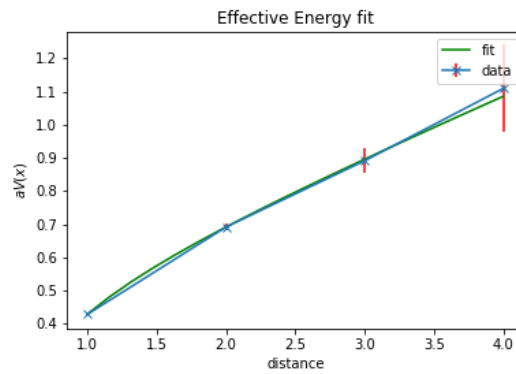


**Figure 4.3:** The Static Quark Potential and fitting model.

increase, which can be a signal of confinement is SU(2) theory. To fit this potential in the form of 2.21, the parameters are:  $A=-0.17(2)$ ,  $B=0.42(3)$ ,  $C=0.17(1)$ .

## 5 Summary

In this project we simulated a SU(2) gauge theory on the lattice, and get the Static Quark Potential via Wilson Loops. We show that the quark potential can be parameterized as

$$V(r) = \frac{-0.17(2)}{r} + 0.42(3) + 0.17(1)r \quad (5.1)$$

Which can be a evidence of Quark Confinement in SU(2) theory.

The main uncertainty comes form sample size, as we can see in 4.2, the 500 sample size is not big enough and give us a huge variance in static potential fitting. But this is just a problem of time, once we run a bigger simulation, we will get a reasonable results.

The theory itself can also be improved. Here we use the simplest gauge action, only consider the smallest loops in the lattice. One can actually use more complex action to improve the accuracy. [2]

We can also do more things on this model. In 2.1 We see that the potential we get is coupled with lattice space  $a$ , which is not determined. We can finish this using the Sommer parameter, which is related with the shape of static quark potential. [1] Till now we just focus on the gauge field, we can also put fermion fields on the lattice and try to get some physical particles, but this is far from our project.

# Bibliography

- [1] Christof Gattringer and Christian B. Lang. Quantum chromodynamics on the lattice. *Lect. Notes Phys.*, 788:1–343, 2010.
- [2] G. Peter Lepage. Lattice qcd for novices, 2005.
- [3] Carsten Urbach. Reversibility violation in the hybrid monte carlo algorithm. *Computer Physics Communications*, 224:44–51, Mar 2018.